Conduction Band Cliff at the CdS/$CuIn_{0.1}Ga_{0.9}Se_2$ Thin-Film Solar Cell Interface

Mary Blankenship[1*], Dirk Hauschild[1, 2, 3], Luisa Both[2,3], Elizaveta Pyatenko[2,3,4], Wolfram Witte[5], Dimitrios Hariskos[5], Stefan Paetel[5], Michael Powalla[5,6], Lothar Weinhardt[1, 2, 3], and Clemens Heske[1, 2, 3*]

[1]Department of Chemistry and Biochemistry, University of Nevada, Las Vegas (UNLV), 4505 Maryland Parkway, Las Vegas, Nevada 89154-4003, United States

[2]Institute for Photon Science and Synchrotron Radiation (IPS), Karlsruhe Institute of Technology (KIT), Hermann-von-Helmholtz-Platz 1, 76344 Eggenstein-Leopoldshafen, Germany

[3]Institute for Chemical Technology and Polymer Chemistry (ITCP), Karlsruhe Institute of Technology (KIT), Engesserstraße 18/20, 76131 Karlsruhe, Germany

[4]Laboratory for Applications of Synchrotron Radiation (LAS), Karlsruhe Institute of Technology (KIT), Kaiserstraße 12, 76131 Karlsruhe, Germany

[5]Zentrum für Sonnenenergie- und Wasserstoff-Forschung Baden-Württemberg (ZSW), Meitnerstraße 1, 70563 Stuttgart, Germany

[6]Light Technology Institute (LTI), Karlsruhe Institute of Technology (KIT), Engesserstraße 13, 76131 Karlsruhe, Germany

*Authors to whom correspondence should be addressed: blankens@unlv.nevada.edu heske@unlv.nevada.edu

KEYWORDS: $Cu(In,Ga)Se_2$, CIGSe, thin-film solar cell, CdS buffer layer, RbF post-deposition treatment, photoelectron spectroscopy, inverse photoemission, electronic structure, wide-gap devices

Abstract

The electronic structure of a Ga-rich wide-gap $CuIn_{0.1}Ga_{0.9}Se_2$ thin-film solar cell absorber and its interface with a solution-grown CdS buffer layer were directly investigated using a combination of x-ray and ultraviolet photoelectron spectroscopy with inverse photoemission spectroscopy. After a state-of-the-art RbF post-deposition treatment, we observe a small amount of Rb at the absorber surface, but no indication of a Rb-(In,Ga)-Se layer. The surface band gap of the absorber is determined to 1.79 (± 0.14) eV, which is approx. 0.2 eV larger than its optical bulk band gap. The special character of the Cu-poor and Rb-containing absorber surface highlights the need for a direct and all-experimental determination of the conduction band. For the $CdS/CuIn_{0.1}Ga_{0.9}Se_2$ interface, we find a significant cliff in the conduction band (-0.53 ± 0.15 eV), which we identify as a limiting factor for the performance of such Ga-rich wide-gap devices.

TOC Graphic

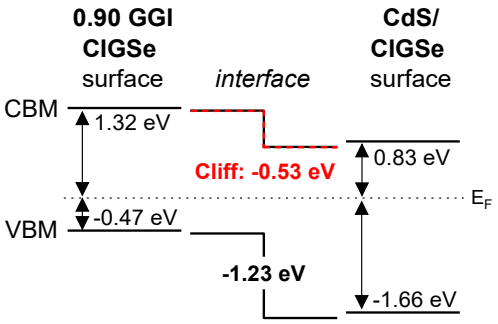

Introduction

Several research groups have shown energy conversion efficiencies above 21% using lab-scale $Cu(In,Ga)(S,Se)_2$-based (CIGSSe) thin-film solar cells.[1–5] Such high efficiencies are achieved with highly optimized devices, including the application of alkali elements (i.e., K, Rb, and Cs) in a post-deposition treatment (PDT) of the CIGSSe or $Cu(In,Ga)Se_2$ (CIGSe) absorber surface.[2,4,6–12] The high-efficiency CIGSe absorbers typically exhibit an integral (bulk) Ga/(Ga+In) (GGI) ratio of ≈ 0.3,[7,8] and have an optically measured bulk band gap (E_g) of roughly 1.1 eV.[13,14]

Despite the high efficiencies achieved for GGI ≈ 0.3, wide band gap chalcopyrite absorbers have recently drawn attention due to higher theoretical open-circuit voltages, their potential uses as a top cell in a tandem solar-cell device[14–16], and in photoelectrochemical water splitting.[17–19] However, cells with high GGI absorbers lead to photovoltaic devices with much lower efficiencies than predicted, mainly caused by an increase of the open-circuit voltage (V_{OC}) deficit (i.e., $E_g/e - V_{OC}$) for increasing GGI.[14,16,20–24] For example, the highest efficiency reported for (In-free) $CdS/CuGaSe_2$-based thin-film solar cells is only 11%.[25]

The combination of high GGI absorbers *and* PDTs (in particular when using heavy alkali elements) is a promising route to increase the efficiency of such devices (see, e.g., Refs.[4,10,26]). While a KF- or RbF-PDT applied to a CIGSe surface with GGI ratios up to ≈ 0.80 can improve V_{OC} by 30-130 mV,[13,27,28] pure In-free $CuGaSe_2$ absorbers did not show any efficiency improvement.[6] For low-gap CIGSe absorbers, an alkali-In-Se_2 surface species has been reported for some PDT treatments,[29–32] while other studies merely found a modification of the electronic structure at the RbF-treated CIGSe surface.[7,8,33] For absorbers with a GGI of ≈ 0.8, a $K(In,Ga)Se_2$ surface layer is only postulated,[28] and no alkali-Ga-Se_2 type bonds were found for In-free $CuGaSe_2$.[28,30] This suggests that the changes induced by the alkali PDT not only strongly depend on the absorber.[12] To further increase the performance of high-GGI CIGSe-based solar cells, it is thus crucial to understand the influence of the PDT on the chemical and electronic structure of such absorber surfaces and the corresponding buffer/absorber interfaces.

Wide-gap CIGSSe-based thin film solar cells have been intensively studied, including the band alignment at the CdS/CIGSSe interface. However, several studies determined the conduction band alignment only *indirectly* using either valence band measurements and bulk band gaps or density functional theory.[34–42] This approach has led to reports or assumptions of roughly estimated or even incorrect conduction band offsets, especially for the CdS/CIGSSe interface with an absorber GGI ≈ 0.3,[43–51] and was rectified by Morkel *et al.* in a *direct* measurement using a combination of x-ray and ultraviolet photoelectron spectroscopy (XPS and UPS, respectively), as well as inverse photoemission spectroscopy (IPES).[52]

In our previous work (2005, Ref.[53]) on the interface between CdS and a wide-gap $Cu(In,Ga)S_2$ (CIGS, i.e., sulfur-based) absorber with GGI ≈ 0.20, we found a nonideal negative conduction band offset, often referred to as "cliff". Such an alignment possibly leads to recombination at the interface and decreases the efficiency of the device (as described in Ref.[53]). While the wide-gap character in the previous work was achieved by replacing Se with S, here we probe *all-experimentally and directly* whether such an unfavorable band alignment also occurs if the wide-gap character is induced by a high Ga content using a combination of XPS, UPS, and IPES. Furthermore, we will shed light on the impact of our state-of-the-art RbF-PDT on the absorber surface before growing the CdS buffer layer with a chemical-bath deposition (CBD).

Methods

The CIGSe absorbers were prepared with an in-line multi-stage process by co-evaporation of Cu, In, Ga, and Se onto a Mo-coated soda-lime glass (SLG) substrate at the ZSW.[54,55] Afterwards, the absorber underwent a RbF-PDT under Se atmosphere without breaking the vacuum, which includes a rinse in a 1.5 M ammonia solution. X-ray fluorescence (XRF) was used to determine a bulk GGI ratio of 0.90 (± 0.02). With external quantum efficiency (EQE) measurements, an optical (bulk) band gap of 1.60 (± 0.01) eV was derived.

CdS buffer layers of two different thicknesses were grown by CBD with a thiourea-based process on top of the CIGSe surface using deposition times of 2 and 8 minutes, which resulted in nominal CdS thicknesses of 3 and 50 nm, respectively. The correlation between deposition time and CdS thickness was estimated and corroborated by a separate study on absorbers with a GGI of ~0.3 using x-ray photoelectron spectroscopy.[56] The 3 nm sample was chosen to still detect signals from the absorber with XPS, whereas the 50 nm sample represents the standard buffer for devices. Sister samples of the ones studied here from the same deposition campaign and same carrier, processed to full solar cells with the 50 nm thick CBD-CdS and an i-ZnO/ZnO:Al front contact, achieved up to 7.5% efficiency and a V_{OC} up to 830 mV, corresponding to a pronounced V_{OC} deficit of 770 mV.

At ZSW, the here-studied samples were briefly exposed to air for less than 5 minutes before being sealed in a dry N_2 environment and shipped to UNLV, where the samples were unpacked, mounted in a nitrogen-filled glovebox, and transferred into an ultra-high vacuum system with a base pressure below 5×10^{-10} mbar (without any additional air exposure).

The XPS and UPS data were measured with a Scienta R4000 electron analyzer (calibrated according to Ref.[57]). A non-monochromatized Mg K_α x-ray source (SPECS XR 50) and a monochromatized Al K_α x-ray source (VG Scienta SAX-100) were used for XPS, while a monochromated He I and II source (Gammadata VUV 5000) was employed for UPS. For the IPES experiments, a STAIB NEK-150-1 low-energy electron gun, a photon detector with a Semrock Hg01-254-25 mercury line filter (central photon energy of 4.88 eV), and a Hamamatsu R6834 photomultiplier were used.[7,58] The Fermi edge of a sputter-cleaned Ag foil was used to calibrate the energy scales for UPS and IPES and for determining the overall energy resolution of ~115 and ~420 meV for UPS and IPES, respectively. After the initial "as-received" XPS, UPS, and IPES dataset was taken, the samples were subjected to 50 eV low-energy Ar^+ ion treatments for up to 4 minutes to reduce the amount of potential surface adsorbates without damaging the sample surface (such as the formation of metallic phases, as observed at higher ion energies or very long ion-beam exposure[52,59,60]).

Results & Discussion

In Figure 1, the XPS survey spectra of the CIGSe absorber, and the 3 and 50 nm CdS/CIGSe samples are shown. The data was taken after 50 eV Ar^+ ion treatments of 4 min for the CIGSe absorber and the 50 nm CdS/CIGSe sample, and 2 min for the 3 nm CdS/CIGSe sample, respectively. The low-energy Ar^+ ion treatment significantly reduces the oxygen- and carbon-related signals, while no formation of unwanted metallic phases at the surface is detected in any of our measurement techniques.

The survey spectrum of the absorber surface exhibits all expected absorber-related peaks (e.g., Ga 2p, Cu 2p, In 3d, and Se 3d), as well as small signals of sodium, likely due to diffusion from the SLG substrate towards the surface.[61] As expected for a CIGSe absorber with a nominal GGI ratio of 0.90, we find only

small indium signals (e.g., In 3d) and large gallium signals (e.g., Ga 2p). The surface GGI ratio is calculated using the In 4d/Ga 3d region by conducting a fit using a linear background, Voigt profiles, and the Fityk software.[62,63] The In 4d- and Ga 3d-derived bands were approximated as shallow core levels and each described by a single peak doublet with fixed Lorentzian and Gaussian widths and a 2:3 peak ratio according to their 2j + 1 multiplicity. After taking the photoionization cross sections into account,[63] we derive a GGI *surface* ratio of 0.93 (± 0.03), which is slightly higher than the bulk GGI of 0.90 (± 0.02) determined by XRF (but well within the error bars).

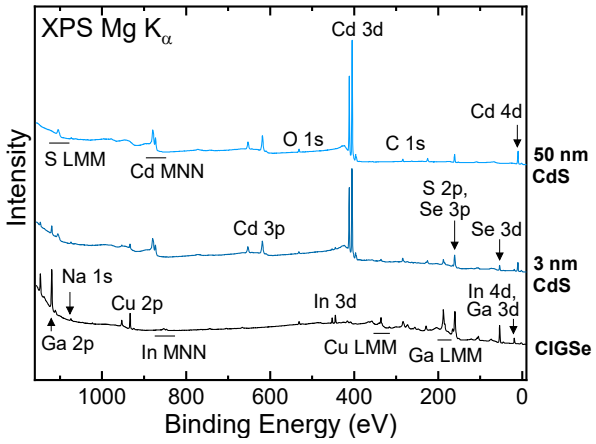

Figure 1. Mg K_α XPS survey spectra of $CuIn_{0.1}Ga_{0.9}Se_2$ absorber with RbF-PDT (black), and 3 and 50 nm CdS/CIGSe samples (blue) after 50 eV Ar^+ ion treatments of 2 min (3 nm sample) or 4 min (other samples). Prominent photoelectron and Auger features are labelled.

We also find trace amounts of fluorine at the surface, likely residuals from the RbF-PDT, which were not completely removed by the NH_3-based rinsing step. The most-prominent XPS rubidium feature (Rb 3d at ~111 eV) overlaps with the Ga 3p peaks; due to the high gallium content, a clear rubidium signal is thus not detectable in our XPS spectra. However, hard x-ray photoelectron spectroscopy data of twin samples, excited with 2.1 keV photons, shows a clear Rb 2p signal (unpublished results). In contrast to some studies on low-gap PDT-treated CIGSe absorbers,[29–32] we find no indications for the formation of an alkali-In-Se layer at the here-investigated indium-poor wide-gap CIGSe surface. Moreover, no evidence for a ternary alkali-Ga-Se environment was found, which is in agreement with reported findings for In-free RbF-PDT-treated $CuGaSe_2$ absorbers.[30] With increasing CdS thickness, the buffer-related peaks increase, while the absorber-related peaks decrease in intensity and fully vanish for the 50 nm CdS/CIGSe sample, indicating a completely closed buffer layer, as intended.

To determine the band edge positions at the interface, the CIGSe absorber and the thickest (i.e., 50 nm) CdS/CIGSe sample were measured with UPS and IPES. Figure 2 shows the corresponding spectra of the two samples after 4 min Ar^+ ion treatment. The valence band maxima (VBMs) and conduction band minima (CBMs) were determined by linear extrapolation of the leading edges.[52,64,65] For the absorber, we find the VBM at -0.47 (± 0.10) eV and the CBM at 1.32 (± 0.10) eV. This result indicates that the band bending towards the high GGI absorber surface is less pronounced than generally found for low GGI absorbers, since the Fermi energy "lies lower" in the band gap.[7,53,58] The absorber *surface* band gap then is calculated to be 1.79 (± 0.14) eV, which is similar to that found at the surface of the above-mentioned pure "sulfide" $Cu(In,Ga)S_2$ (CIGS) absorber with a GGI of ~0.20.[53] The surface band gap is larger than the

bulk band gap of 1.60 (± 0.01) eV derived from external quantum efficiency (EQE) measurements. Such a difference between bulk and surface band gap is a common finding in well-performing chalcopyrite solar cells[44,52,66] and is mostly attributed to a Cu-depletion at the absorber surface. We have also determined the Cu/(Ga+In) (CGI) ratio at the surface of the high-GGI absorber, using the Cu 3p, In 4d, and Ga 3d lines and the corresponding photoionization cross sections,[63] and find a value of 0.4 (± 0.1). This value is significantly smaller than the nominal bulk value of ~0.7, but similar to the one found for Cu(In,Ga)Se_2 with a GGI of 0.3 [i.e., 0.34 (±0.09)].[8]

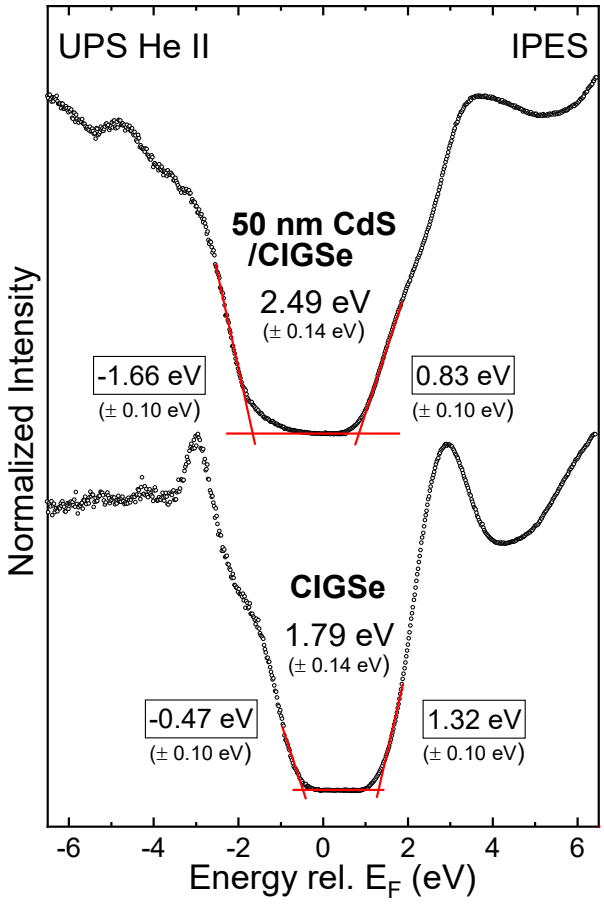

Figure 2. He II UPS (left) and IPES (right) spectra with respect to the Fermi energy (E_F) of the $CuIn_{0.1}Ga_{0.9}Se_2$ absorber with RbF-PDT and the 50 nm CdS/CIGSe sample after 4 min of 50 eV Ar^+-ion treatment. The VBM and CBM given in the boxes were determined using a linear extrapolation of the leading edges, as indicated by the red lines. The derived surface band gaps are also shown.

The VBM and CBM of the 50 nm CdS/CIGSe sample are -1.66 eV and 0.83 eV, respectively. The valence band of the 50 nm CdS/CIGSe sample exhibits a rather large tail (at ~ -1.3 eV), which is not described by the linear extrapolation. Such a tail is rather uncommon for CdS buffers in high-efficiency devices, where no or only a small tail can generally be found in the valence band spectra.[7,52,53,66,67] We speculate that this is due to a rather high defect state density of the CdS buffer layer on high-GGI CIGSe surfaces.[67,68] Nevertheless, the band gap of 2.49 (± 0.14) eV at the CdS surface is similar to previously reported values for CBD-CdS surfaces.[7,52,53] In a first approximation, the direct comparison of the conduction band minima of the CIGSe absorber and the 50 nm CdS/CIGSe sample indicates a cliff-like conduction band alignment.

For a more precise determination of the band alignment at the interface, changes of the band bending induced by the formation of the buffer-absorber interface need to be taken into account as well.

Table 1. XPS core-level binding energies and the derived corrections for the interface-induced band bending using the $CuIn_{0.1}Ga_{0.9}Se_2$ absorber with RbF-PDT, 50 nm CdS/CIGSe, and the 3 nm CdS/CIGSe sample.

Core level	Cu $2p_{3/2}$ (eV)	In $3d_{3/2}$ (eV)	Ga $2p_{3/2}$ (eV)	Se $3d_{5/2}$ (eV)	Average shift (eV)	Core level	Cd $3d_{3/2}$ (eV)	S $2p_{3/2}$ (eV)	Average shift (eV)
CIGSe	932.56	452.59	1118.14	54.18		50 nm CdS/CIGSe	412.03	161.47	
3 nm CdS/CIGSe	932.66	452.58	1118.19	54.20		3 nm CdS/CIGSe	412.16	161.50	
Shift	-0.10	0.01	-0.05	-0.02	**- 0.04 ± 0.05**	Shift	-0.13	-0.03	**- 0.08 ± 0.07**

To determine this correction, we used the 3 nm CdS/CIGSe sample, for which both absorber and buffer-related photoelectron lines are present, to monitor the *relative* shifts of the absorber core levels (Cu $2p_{3/2}$, In $3d_{3/2}$, Ga $2p_{3/2}$, and Se $3d_{5/2}$) as well as the CdS buffer layer core levels (Cd $3d_{3/2}$ and S $2p_{3/2}$). The binding energies of Se $3d_{5/2}$ and S $2p_{3/2}$, listed in Table 1, were derived by fitting these regions with linear backgrounds and spin-orbit-split peak doublets. We calculate an average shift of -0.04 (± 0.05) eV for the absorber core levels and -0.08 (± 0.07) eV for buffer-related core levels. The negligible additional shift of the absorber-related core levels might indicate that the Fermi level is pinned, suggesting a high defect concentration at the interface.[69] This is typically accompanied with increased interface recombination and a drop in the open-circuit voltage V_{OC}.[40,43,69] The presence of defects at the interface is corroborated by the observation of a significant valence-band tail in the CdS UPS spectrum, which suggests that such interfacial defects can lead to a poorer buffer layer growth with an increased number of defects in the CdS buffer layer itself.

The VBM and CBM values, combined with the corrections for interface-induced band bending to derive the band alignment, are shown in Figure 3. We find a significant cliff in the conduction band, with an offset of -0.53 (± 0.15) eV, and a valence band offset of -1.23 (± 0.15) eV. This is an unfavorable alignment, as the presence of such a significant cliff (-0.53 eV) severely impacts the balance between charge-carrier transport across, and recombination at, the interface. This, in turn, is expected to lead to interface recombination and limit the V_{OC} [53,70–72] (due to the large V_{OC} deficit well above 700 mV). In the current study, we observe a sizable cliff in the conduction band, similar to that at the interface between CdS and wide-gap, pure-sulfur CIGS.[53]

To remedy the situation, three steps can be proposed that would impact the properties of the interface in question. First, further optimization of the CBD-CdS deposition *for this particular* wide-gap surface composition could be pursued (e.g., by testing regions of parameter space that have not proven successful for low-gap absorbers). This could possibly lead to a reduced presence of interface defects and thus reduce the likelihood of Fermi level pinning. In turn, this would allow for an additional downward band bending of the CIGSe absorber towards the surface (i.e., a downward shift of the band edges) upon interface formation.[73] Second, the buffer material could also be modified, either in doping character, or, likely more promising, in overall composition and band gap.[24] A wider band gap could lead to a higher

CBM position in the buffer and possibly reduce the magnitude of the conduction band cliff, which was shown to be a promising route by Larsson *et al.* using $Zn_{1-x}Sn_xO_y$.[15] And third, the RbF-PDT could be optimized for this interface, which might lead to a decrease of interface recombination (as observed for low band gap absorbers[2,11,74,75]).

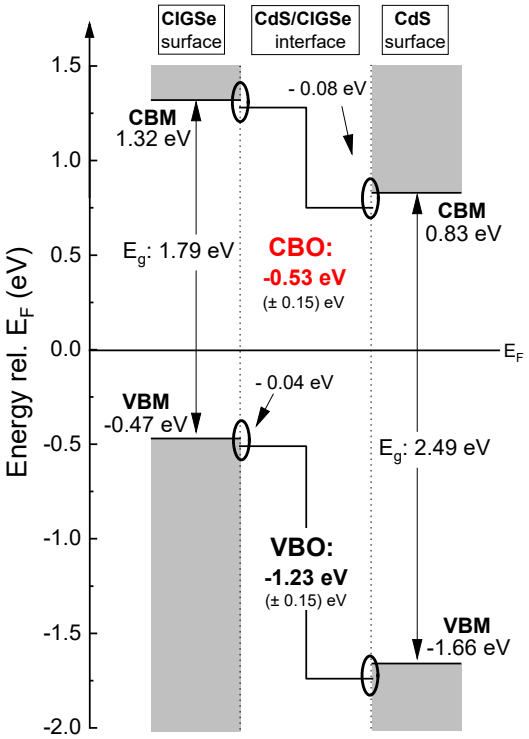

Figure 3. Schematic band alignment at the CdS/RbF-PDT high GGI CIGSe interface. The determined band edges are shown for the $CuIn_{0.1}Ga_{0.9}Se_2$ absorber and the 50 nm CBD-CdS buffer surfaces. The derived conduction band offset (CBO, shown in red) and valence band offset (VBO) include the correction for interface-induced band bending.

Conclusions

We have investigated the electronic structure of the interface between a high Ga/(Ga+In) ratio (wide-gap) RbF-treated $Cu(In,Ga)Se_2$ absorber and a solution-grown CdS buffer layer using XPS, UPS, and IPES. We derive a GGI ratio of 0.93 (± 0.03) at the absorber surface, compared to 0.90 (± 0.02) in the bulk. The electronic surface band gap is determined as 1.79 (± 0.14) eV, which is ~0.2 eV larger than the optical bulk band gap. We surmise that the Cu-depleted surface stoichiometry causes this band gap widening, similar to CIGSe absorbers with a GGI of 0.3 eV, which re-emphasizes the importance of investigating the real interface. At the CdS/Ga-rich wide-gap $CuIn_{0.1}Ga_{0.9}Se_2$ interface, we find that the Fermi level is pinned, likely due to interface defects that also induce defect states in the valence band of the CdS buffer. We derive a VBO of -1.23 (± 0.15) eV and observe a significant cliff (-0.53 ± 0.15 eV) in the conduction band alignment. This unfavorable band alignment leads to strong interface recombination, which likely limits the V_{OC}. This direct and all-experimental determination of the band alignment refines earlier publications

that only used indirect methods, e.g., surface valence band values and optical (bulk) band gaps, temperature-dependent J-V measurements combined with simulations, or theory. In future, a re-optimization or replacement of the buffer layer and/or possibly an adjustment of the PDT could remedy our findings.

ACKNOWLEDGMENTS

The authors are grateful for financial support by the German Federal Ministry for Economic Affairs and Climate Action (BMWK) in projects “EFFCIS” (Nos. 0324076A and 0324076E) and “EFFCIS-II” (Nos. 03EE1059A and 03EE1059E).

REFERENCES

(1) Nakamura, M.; Yamaguchi, K.; Kimoto, Y.; Yasaki, Y.; Kato, T.; Sugimoto, H. Cd-Free Cu(In,Ga)(Se,S)$_2$ Thin-Film Solar Cell With Record Efficiency of 23.35%. *IEEE J. Photovolt.* **2019**, *9* (6), 1863–1867. https://doi.org/10.1109/JPHOTOV.2019.2937218.

(2) Jackson, P.; Wuerz, R.; Hariskos, D.; Lotter, E.; Witte, W.; Powalla, M. Effects of Heavy Alkali Elements in Cu(In,Ga)Se$_2$ Solar Cells with Efficiencies up to 22.6%. *Phys. Status Solidi RRL – Rapid Res. Lett.* **2016**, *10* (8), 583–586. https://doi.org/10.1002/pssr.201600199.

(3) Siebentritt, S.; Avancini, E.; Bär, M.; Bombsch, J.; Bourgeois, E.; Buecheler, S.; Carron, R.; Castro, C.; Duguay, S.; Félix, R.; et al. Heavy Alkali Treatment of Cu(In,Ga)Se$_2$ Solar Cells: Surface versus Bulk Effects. *Adv. Energy Mater.* **2020**, *10* (8), 1903752. https://doi.org/10.1002/aenm.201903752.

(4) Jackson, P.; Hariskos, D.; Wuerz, R.; Kiowski, O.; Bauer, A.; Friedlmeier, T. M.; Powalla, M. Properties of Cu(In,Ga)Se$_2$ Solar Cells with New Record Efficiencies up to 21.7%. *Phys. Status Solidi RRL – Rapid Res. Lett.* **2015**, *9* (1), 28–31. https://doi.org/10.1002/pssr.201409520.

(5) *Empa - Communication - CIGS-efficiency-record-2021*. https://www.empa.ch/web/s604/cigs-efficiency-record-2021 (accessed 2022-02-07).

(6) Ishizuka, S. CuGaSe$_2$ Thin Film Solar Cells: Challenges for Developing Highly Efficient Wide-Gap Chalcopyrite Photovoltaics. *Phys. Status Solidi A* **2019**, *216* (15), 1800873. https://doi.org/10.1002/pssa.201800873.

(7) Hauschild, D.; Kreikemeyer-Lorenzo, D.; Jackson, P.; Friedlmeier, T. M.; Hariskos, D.; Reinert, F.; Powalla, M.; Heske, C.; Weinhardt, L. Impact of a RbF Postdeposition Treatment on the Electronic Structure of the CdS/Cu(In,Ga)Se$_2$ Heterojunction in High-Efficiency Thin-Film Solar Cells. *ACS Energy Lett.* **2017**, *2* (10), 2383–2387. https://doi.org/10.1021/acsenergylett.7b00720.

(8) Kreikemeyer-Lorenzo, D.; Hauschild, D.; Jackson, P.; Friedlmeier, T. M.; Hariskos, D.; Blum, M.; Yang, W.; Reinert, F.; Powalla, M.; Heske, C.; et al. Rubidium Fluoride Post-Deposition Treatment: Impact on the Chemical Structure of the Cu(In,Ga)Se$_2$ Surface and CdS/Cu(In,Ga)Se$_2$ Interface in Thin-Film Solar Cells. *ACS Appl. Mater. Interfaces* **2018**, *10* (43), 37602–37608. https://doi.org/10.1021/acsami.8b10005.

(9) Mezher, M.; Mansfield, L. M.; Horsley, K.; Blum, M.; Wieting, R.; Weinhardt, L.; Ramanathan, K.; Heske, C. KF Post-Deposition Treatment of Industrial Cu(In, Ga)(S, Se)$_2$ Thin-Film Surfaces: Modifying the Chemical and Electronic Structure. *Appl. Phys. Lett.* **2017**, *111* (7), 071601. https://doi.org/10.1063/1.4998445.

(10) Chirilă, A.; Reinhard, P.; Pianezzi, F.; Bloesch, P.; Uhl, A. R.; Fella, C.; Kranz, L.; Keller, D.; Gretener, C.; Hagendorfer, H.; et al. Potassium-Induced Surface Modification of Cu(In,Ga)Se$_2$ Thin Films for High-Efficiency Solar Cells. *Nat. Mater.* **2013**, *12* (12), 1107–1111. https://doi.org/10.1038/nmat3789.

(11) Pianezzi, F.; Reinhard, P.; Chirilă, A.; Bissig, B.; Nishiwaki, S.; Buecheler, S.; Tiwari, A. N. Unveiling the Effects of Post-Deposition Treatment with Different Alkaline Elements on the Electronic Properties of CIGS Thin Film Solar Cells. *Phys. Chem. Chem. Phys.* **2014**, *16* (19), 8843–8851. https://doi.org/10.1039/C4CP00614C.

(12) Ishizuka, S.; Taguchi, N.; Nishinaga, J.; Kamikawa, Y.; Tanaka, S.; Shibata, H. Group III Elemental Composition Dependence of RbF Postdeposition Treatment Effects on Cu(In,Ga)Se$_2$ Thin Films and Solar Cells. *J. Phys. Chem. C* **2018**, *122* (7), 3809–3817. https://doi.org/10.1021/acs.jpcc.8b00079.

(13) Pistor, P.; Greiner, D.; Kaufmann, C. A.; Brunken, S.; Gorgoi, M.; Steigert, A.; Calvet, W.; Lauermann, I.; Klenk, R.; Unold, T.; et al. Experimental Indication for Band Gap Widening of

Chalcopyrite Solar Cell Absorbers after Potassium Fluoride Treatment. *Appl. Phys. Lett.* **2014**, *105* (6), 063901. https://doi.org/10.1063/1.4892882.
(14) Contreras, M. A.; Mansfield, L. M.; Egaas, B.; Li, J.; Romero, M.; Noufi, R.; Rudiger-Voigt, E.; Mannstadt, W. Wide Bandgap Cu(In,Ga)Se_2 Solar Cells with Improved Energy Conversion Efficiency. *Prog. Photovolt. Res. Appl.* **2012**, *20* (7), 843–850. https://doi.org/10.1002/pip.2244.
(15) Larsson, F.; Nilsson, N. S.; Keller, J.; Frisk, C.; Kosyak, V.; Edoff, M.; Törndahl, T. Record 1.0 V Open-Circuit Voltage in Wide Band Gap Chalcopyrite Solar Cells. *Prog. Photovolt. Res. Appl.* **2017**, *25* (9), 755–763. https://doi.org/10.1002/pip.2914.
(16) Zahedi-Azad, S.; Scheer, R. Quenching Interface Recombination in Wide Bandgap Cu(In,Ga)Se_2 by Potassium Treatment. *Phys. Status Solidi C* **2017**, *14* (6), 1600203. https://doi.org/10.1002/pssc.201600203.
(17) Carter, J. C.; Hauschild, D.; Weinhardt, L.; Horsley, K.; Hariskos, D.; Gaillard, N.; Heske, C. Electronic Structure of Chalcopyrite Surfaces for Photoelectrochemical Hydrogen Production. *J. Phys. Chem. C* **2023**, *127* (17), 8235–8246. https://doi.org/10.1021/acs.jpcc.2c09063.
(18) Jacobsson, T. J.; Fjällström, V.; Edoff, M.; Edvinsson, T. Sustainable Solar Hydrogen Production: From Photoelectrochemical Cells to PV-Electrolyzers and Back Again. *Energy Env. Sci* **2014**, *7* (7), 2056–2070. https://doi.org/10.1039/C4EE00754A.
(19) Jacobsson, T. J.; Platzer-Björkman, C.; Edoff, M.; Edvinsson, T. CuInxGa1−xSe2 as an Efficient Photocathode for Solar Hydrogen Generation. *Int. J. Hydrog. Energy* **2013**, *38* (35), 15027–15035. https://doi.org/10.1016/j.ijhydene.2013.09.094.
(20) Schock, H. W.; Rau, U.; Hanna, G.; Balboul, M.; Margorian-Friedlmeier, T.; Jasenek, A.; Kötschau, I.; Kerber, H.; Wiesner, H. High Efficiency, High Voltage Solar Cells by Band Gap and Defect Engineering in Cu(In,Ga)$(S,Se)_2$ Chalcopyrite Semiconductors; 16th European Photovoltaic Solar Energy Conference, Glasgow, Scotland, 2000.
(21) Herberholz, R.; Nadenau, V.; Rühle, U.; Köble, C.; Schock, H. W.; Dimmler, B. Prospects of Wide-Gap Chalcopyrites for Thin Film Photovoltaic Modules. *Sol. Energy Mater. Sol. Cells* **1997**, *49* (1), 227–237. https://doi.org/10.1016/S0927-0248(97)00199-2.
(22) Ott, N.; Strunk, H. P.; Albrecht, M.; Hanna, G.; Kniese, R. Electro-Optical Properties of the Microstructure in Chalcopyrite Thin Films. In *Wide-Gap Chalcopyrites*; Siebentritt, S., Rau, U., Eds.; Springer Series in Materials Science; Springer: Berlin, Heidelberg, 2006; pp 179–191. https://doi.org/10.1007/3-540-31293-5_9.
(23) Ishizuka, S. Impact of Cu-Deficient p-n Heterointerface in $CuGaSe_2$ Photovoltaic Devices. *Appl. Phys. Lett.* **2021**, *118* (13), 133901. https://doi.org/10.1063/5.0047062.
(24) Turcu, M.; Pakma, O.; Rau, U. Interdependence of Absorber Composition and Recombination Mechanism in Cu(In,Ga)$(Se,S)_2$ Heterojunction Solar Cells. *Appl. Phys. Lett.* **2002**, *80* (14), 2598–2600. https://doi.org/10.1063/1.1467621.
(25) Ishizuka, S.; Yamada, A.; Fons, P. J.; Shibata, H.; Niki, S. Impact of a Binary Ga_2Se_3 Precursor on Ternary $CuGaSe_2$ Thin-Film and Solar Cell Device Properties. *Appl. Phys. Lett.* **2013**, *103* (14), 143903. https://doi.org/10.1063/1.4823585.
(26) Eslam, A.; Wuerz, R.; Hauschild, D.; Weinhardt, L.; Hempel, W.; Powalla, M.; Heske, C. Impact of Substrate Temperature during NaF and KF Post-Deposition Treatments on Chemical and Optoelectronic Properties of Alkali-Free Cu(In,Ga)Se_2 Thin Film Solar Cell Absorbers. *Thin Solid Films* **2021**, *739*, 138979. https://doi.org/10.1016/j.tsf.2021.138979.
(27) Zahedi-Azad, S.; Maiberg, M.; Clausing, R.; Scheer, R. Influence of Heavy Alkali Post Deposition Treatment on Wide Gap Cu(In,Ga)Se_2. *Thin Solid Films* **2019**, *669*, 629–632. https://doi.org/10.1016/j.tsf.2018.11.041.

(28) Zahedi-Azad, S.; Maiberg, M.; Scheer, R. Effect of Na-PDT and KF-PDT on the Photovoltaic Performance of Wide Bandgap Cu(In,Ga)Se_2 Solar Cells. *Prog. Photovolt. Res. Appl.* **2020**, *28* (11), 1146–1157. https://doi.org/10.1002/pip.3317.

(29) Handick, E.; Reinhard, P.; Wilks, R. G.; Pianezzi, F.; Kunze, T.; Kreikemeyer-Lorenzo, D.; Weinhardt, L.; Blum, M.; Yang, W.; Gorgoi, M.; et al. Formation of a K—In—Se Surface Species by NaF/KF Postdeposition Treatment of Cu(In,Ga)Se_2 Thin-Film Solar Cell Absorbers. *ACS Appl. Mater. Interfaces* **2017**, *9* (4), 3581–3589. https://doi.org/10.1021/acsami.6b11892.

(30) Taguchi, N.; Tanaka, S.; Ishizuka, S. Direct Insights into $RbInSe_2$ Formation at Cu(In,Ga)Se_2 Thin Film Surface with RbF Postdeposition Treatment. *Appl. Phys. Lett.* **2018**, *113* (11), 113903. https://doi.org/10.1063/1.5044244.

(31) Lepetit, T.; Harel, S.; Arzel, L.; Ouvrard, G.; Barreau, N. KF Post Deposition Treatment in Co-Evaporated Cu(In,Ga)Se_2 Thin Film Solar Cells: Beneficial or Detrimental Effect Induced by the Absorber Characteristics. *Prog. Photovolt. Res. Appl.* **2017**, *25* (12), 1068–1076. https://doi.org/10.1002/pip.2924.

(32) Bombsch, J.; Avancini, E.; Carron, R.; Handick, E.; Garcia-Diez, R.; Hartmann, C.; Félix, R.; Ueda, S.; Wilks, R. G.; Bär, M. NaF/RbF-Treated Cu(In,Ga)Se_2 Thin-Film Solar Cell Absorbers: Distinct Surface Modifications Caused by Two Different Types of Rubidium Chemistry. *ACS Appl. Mater. Interfaces* **2020**, *12* (31), 34941–34948. https://doi.org/10.1021/acsami.0c08794.

(33) Nicoara, N.; Kunze, T.; Jackson, P.; Hariskos, D.; Duarte, R. F.; Wilks, R. G.; Witte, W.; Bär, M.; Sadewasser, S. Evidence for Chemical and Electronic Nonuniformities in the Formation of the Interface of RbF-Treated Cu(In,Ga)Se_2 with CdS. *ACS Appl. Mater. Interfaces* **2017**, *9* (50), 44173–44180. https://doi.org/10.1021/acsami.7b12448.

(34) Klein, A. Energy Band Alignment in Chalcogenide Thin Film Solar Cells from Photoelectron Spectroscopy. *J. Phys. Condens. Matter* **2015**, *27* (13), 134201. https://doi.org/10.1088/0953-8984/27/13/134201.

(35) Zhang, S. B.; Wei, S.-H.; Zunger, A. A Phenomenological Model for Systematization and Prediction of Doping Limits in II–VI and I–III–VI_2 Compounds. *J. Appl. Phys.* **1998**, *83* (6), 3192–3196. https://doi.org/10.1063/1.367120.

(36) Schulmeyer, T.; Hunger, R.; Fritsche, R.; Jäckel, B.; Jaegermann, W.; Klein, A.; Kniese, R.; Powalla, M. Interfaces of Chalcogenide Solar Cells: A Study of the Composition at the Cu(In,Ga)Se_2/CdS Contact. *Thin Solid Films* **2005**, *480–481*, 110–117. https://doi.org/10.1016/j.tsf.2004.11.021.

(37) Lany, S.; Zunger, A. Intrinsic DX Centers in Ternary Chalcopyrite Semiconductors. *Phys. Rev. Lett.* **2008**, *100* (1), 016401. https://doi.org/10.1103/PhysRevLett.100.016401.

(38) Gloeckler, M.; Sites, J. R. Efficiency Limitations for Wide-Band-Gap Chalcopyrite Solar Cells. *Thin Solid Films* **2005**, *480–481*, 241–245. https://doi.org/10.1016/j.tsf.2004.11.018.

(39) Siebentritt, S. Wide Gap Chalcopyrites: Material Properties and Solar Cells. *Thin Solid Films* **2002**, *403–404*, 1–8. https://doi.org/10.1016/S0040-6090(01)01525-5.

(40) Klenk, R. Characterisation and Modelling of Chalcopyrite Solar Cells. *Thin Solid Films* **2001**, *387* (1), 135–140. https://doi.org/10.1016/S0040-6090(00)01736-3.

(41) Keller, J.; Sopiha, K. V.; Stolt, O.; Stolt, L.; Persson, C.; Scragg, J. J. S.; Törndahl, T.; Edoff, M. Wide-Gap (Ag,Cu)(In,Ga)Se_2 Solar Cells with Different Buffer Materials—A Path to a Better Heterojunction. *Prog. Photovolt. Res. Appl.* **2020**, *28* (4), 237–250. https://doi.org/10.1002/pip.3232.

(42) Nadenau, V.; Rau, U.; Jasenek, A.; Schock, H. W. Electronic Properties of $CuGaSe_2$-Based Heterojunction Solar Cells. Part I. Transport Analysis. *J. Appl. Phys.* **2000**, *87* (1), 584–593. https://doi.org/10.1063/1.371903.

(43) Minemoto, T.; Matsui, T.; Takakura, H.; Hamakawa, Y.; Negami, T.; Hashimoto, Y.; Uenoyama, T.; Kitagawa, M. Theoretical Analysis of the Effect of Conduction Band Offset of Window/CIS Layers

on Performance of CIS Solar Cells Using Device Simulation. *Sol. Energy Mater. Sol. Cells* **2001**, *67* (1), 83–88. https://doi.org/10.1016/S0927-0248(00)00266-X.
(44) Schmid, D.; Ruckh, M.; Grunwald, F.; Schock, H. W. Chalcopyrite/Defect Chalcopyrite Heterojunctions on the Basis of $CuInSe_2$. *J. Appl. Phys.* **1993**, *73* (6), 2902–2909. https://doi.org/10.1063/1.353020.
(45) Okano, Y.; Nakada, T.; Kunioka, A. XPS Analysis of CdS/$CuInSe_2$ Heterojunctions. *Sol. Energy Mater. Sol. Cells* **1998**, *50* (1), 105–110. https://doi.org/10.1016/S0927-0248(97)00129-3.
(46) Niemegeers, A.; Burgelman, M.; Devos, A. On the CdS/$CuInSe_2$ Conduction-Band Discontinuity. *Appl. Phys. Lett.* **1995**, *67* (6), 843–845.
(47) Burgelman, M.; Nollet, P.; Degrave, S. Modelling Polycrystalline Semiconductor Solar Cells. *Thin Solid Films* **2000**, *361–362*, 527–532. https://doi.org/10.1016/S0040-6090(99)00825-1.
(48) Niemegeers, A.; Burgelman, M.; Decock, K.; Degrave, S.; Verschraegen, J. *Simulation programme SCAPS-1D for thin film solar cells developed at ELIS, University of Gent*. https://scaps.elis.ugent.be/ (accessed 2023-06-21).
(49) Wei, S.; Zunger, A. Band Offsets at the CdS/$CuInSe_2$ Heterojunction. *Appl. Phys. Lett.* **1993**, *63* (18), 2549–2551. https://doi.org/10.1063/1.110429.
(50) Löher, T.; Jaegermann, W.; Pettenkofer, C. Formation and Electronic Properties of the CdS/$CuInSe_2$ (011) Heterointerface Studied by Synchrotron-induced Photoemission. *J. Appl. Phys.* **1995**, *77* (2), 731–738. https://doi.org/10.1063/1.359583.
(51) Nelson, A. J.; Niles, D. W.; Schwerdtfeger, C. R.; Wei, S.-H.; Zunger, A.; Höchst, H. Prediction and Observation of II–VI/$CuInSe_2$ Heterojunction Band Offsets. *J. Electron Spectrosc. Relat. Phenom.* **1994**, *68*, 185–193. https://doi.org/10.1016/0368-2048(94)02116-3.
(52) Morkel, M.; Weinhardt, L.; Lohmüller, B.; Heske, C.; Umbach, E.; Riedl, W.; Zweigart, S.; Karg, F. Flat Conduction-Band Alignment at the CdS/$CuInSe_2$ Thin-Film Solar-Cell Heterojunction. *Appl. Phys. Lett.* **2001**, *79* (27), 4482–4484. https://doi.org/10.1063/1.1428408.
(53) Weinhardt, L.; Fuchs, O.; Groß, D.; Storch, G.; Umbach, E.; Dhere, N. G.; Kadam, A. A.; Kulkarni, S. S.; Heske, C. Band Alignment at the CdS/Cu(In,Ga)S_2 Interface in Thin-Film Solar Cells. *Appl. Phys. Lett.* **2005**, *86* (6), 062109. https://doi.org/10.1063/1.1861958.
(54) Voorwinden, G.; Kniese, R.; Jackson, P.; Powalla, M. IN-LINE Cu(In,Ga)Se_2 CO-EVAPORATION PROCESS ON 30 Cm × 30 Cm SUBSTRATES WITH MULTIPLE DEPOSITION STAGES; 22nd European Photovoltaic Solar Energy Conference, Milan, Italy, 2007.
(55) Gutzler, R.; Witte, W.; Kanevce, A.; Hariskos, D.; Paetel, S. VOC-Losses across the Band Gap: Insights from a High-Throughput Inline Process for CIGS Solar Cells. *Prog. Photovolt. Res. Appl.* **2023**, *31* (10), 1023–1031. https://doi.org/10.1002/pip.3707.
(56) Hauschild, D.; Steininger, R.; Hariskos, D.; Witte, W.; Tougaard, S.; Heske, C.; Weinhardt, L. Using the Inelastic Background in Hard X-Ray Photoelectron Spectroscopy for a Depth-Resolved Analysis of the CdS/Cu(In,Ga)Se_2 Interface. *J. Vac. Sci. Technol. A* **2021**, *39* (6), 063216. https://doi.org/10.1116/6.0001336.
(57) Moulder, J.; Stickle, W.; Sobol, W.; Bomben, K. D. *Handbook of X-Ray Photoelectron Spectroscopy*; Perkin-Elmer Corporation.; Physical Electronics Division: Eden Prairie, MN, 1992.
(58) Yoshida, H. Near-Ultraviolet Inverse Photoemission Spectroscopy Using Ultra-Low Energy Electrons. *Chem. Phys. Lett.* **2012**, *539–540*, 180–185. https://doi.org/10.1016/j.cplett.2012.04.058.
(59) Weinhardt, L.; Blum, M.; Bär, M.; Heske, C.; Cole, B.; Marsen, B.; Miller, E. L. Electronic Surface Level Positions of WO_3 Thin Films for Photoelectrochemical Hydrogen Production. *J. Phys. Chem. C* **2008**, *112* (8), 3078–3082. https://doi.org/10.1021/jp7100286.
(60) van Maris, V. R.; Hauschild, D.; Niesen, T. P.; Eraerds, P.; Dalibor, T.; Palm, J.; Blum, M.; Yang, W.; Heske, C.; Weinhardt, L. Impact of UV-Induced Ozone and Low-Energy Ar^+-Ion Cleaning on the

Chemical Structure of Cu(In,Ga)(S,Se)$_2$ Absorber Surfaces. *J. Appl. Phys.* **2020**, *128* (15), 155301. https://doi.org/10.1063/5.0020253.
(61) Heske, C.; Eich, D.; Fink, R.; Umbach, E.; van Buuren, T.; Bostedt, C.; Kakar, S.; Terminello, L. J.; Grush, M. M.; Callcott, T. A.; et al. Semi-Quantitative and Non-Destructive Analysis of Impurities at a Buried Interface: Na and the CdS/Cu(In,Ga)Se$_2$ Heterojunction. *Surf. Interface Anal.* **2000**, *30* (1), 459–463. https://doi.org/10.1002/1096-9918(200008)30:1<459::AID-SIA757>3.0.CO;2-L.
(62) Wojdyr, M. Fityk: A General-Purpose Peak Fitting Program. *J. Appl. Crystallogr.* **2010**, *43* (5), 1126–1128. https://doi.org/10.1107/S0021889810030499.
(63) Yeh, J. J.; Lindau, I. Atomic Subshell Photoionization Cross Sections and Asymmetry Parameters: 1 ⩽ Z ⩽ 103. *At. Data Nucl. Data Tables* **1985**, *32* (1), 1–155. https://doi.org/10.1016/0092-640X(85)90016-6.
(64) Weinhardt, L.; Hauschild, D.; Heske, C. Surface and Interface Properties in Thin-Film Solar Cells: Using Soft X-Rays and Electrons to Unravel the Electronic and Chemical Structure. *Adv. Mater.* **2019**, *31* (26), 1806660. https://doi.org/10.1002/adma.201806660.
(65) Gleim, T.; Heske, C.; Umbach, E.; Schumacher, C.; Gundel, S.; Faschinger, W.; Fleszar, A.; Ammon, C.; Probst, M.; Steinrück, H.-P. Formation of the ZnSe/(Te/)GaAs(100) Heterojunction. *Surf. Sci.* **2003**, *531* (1), 77–85. https://doi.org/10.1016/S0039-6028(03)00439-4.
(66) Weinhardt, L.; Morkel, M.; Gleim, Th.; Zweigart, S.; Niesen, T. P.; Karg, F.; Heske, C.; Umbach, E. Band Alignment at the CdS/CuIn(S,Se)$_2$ Heterojunction in Thin Film Solar Cells; 2001; p 1261.
(67) Weinhardt, L.; Heske, C.; Umbach, E.; Niesen, T. P.; Visbeck, S.; Karg, F. Band Alignment at the I-ZnO/CdS Interface in Cu(In,Ga)(S,Se)$_2$ Thin-Film Solar Cells. *Appl. Phys. Lett.* **2004**, *84* (16), 3175–3177. https://doi.org/10.1063/1.1704877.
(68) Duncan, D. A.; Mendelsberg, R.; Mezher, M.; Horsley, K.; Rosenberg, S. G.; Blum, M.; Xiong, G.; Weinhardt, L.; Gloeckler, M.; Heske, C. A New Look at the Electronic Structure of Transparent Conductive Oxides—A Case Study of the Interface between Zinc Magnesium Oxide and Cadmium Telluride. *Adv. Mater. Interfaces* **2016**, *3* (22), 1600418. https://doi.org/10.1002/admi.201600418.
(69) Gaillard, N.; Septina, W.; Varley, J.; Ogitsu, T.; Ohtaki, K. K.; Ishii, H. A.; Bradley, J. P.; Muzzillo, C.; Zhu, K.; Babbe, F.; Cooper, J. Performance and Limits of 2.0 EV Bandgap CuInGaS$_2$ Solar Absorber Integrated with CdS Buffer on F:SnO$_2$ Substrate for Multijunction Photovoltaic and Photoelectrochemical Water Splitting Devices. *Mater. Adv.* **2021**, *2* (17), 5752–5763. https://doi.org/10.1039/D1MA00570G.
(70) Bär, M.; Schubert, B.-A.; Marsen, B.; Wilks, R. G.; Pookpanratana, S.; Blum, M.; Krause, S.; Unold, T.; Yang, W.; Weinhardt, L.; et al. Cliff-like Conduction Band Offset and KCN-Induced Recombination Barrier Enhancement at the CdS/Cu$_2$ZnSnS$_4$ Thin-Film Solar Cell Heterojunction. *Appl. Phys. Lett.* **2011**, *99* (22), 222105. https://doi.org/10.1063/1.3663327.
(71) Yamada, A.; Matsubara, K.; Sakurai, K.; Ishizuka, S.; Tampo, H.; Fons, P. J.; Iwata, K.; Niki, S. Effect of Band Offset on the Open Circuit Voltage of Heterojunction CuIn$_{1-x}$Ga$_x$Se$_2$ Solar Cells. *Appl. Phys. Lett.* **2004**, *85* (23), 5607–5609. https://doi.org/10.1063/1.1831566.
(72) Tsoulka, P.; Rivalland, A.; Arzel, L.; Barreau, N. Improved CuGaSe$_2$ Absorber Properties through a Modified Co-Evaporation Process. *Thin Solid Films* **2020**, *709*, 138224. https://doi.org/10.1016/j.tsf.2020.138224.
(73) Caballero, R.; Siebentritt, S.; Kaufmann, C. A.; Kelch, C.; Schweigert, D.; Unold, T.; Rusu, M.; Schock, H.-W.; Lux-Steiner, M. C. CuGaSe$_2$-Based Solar Cells with High Open Circuit Voltage. *MRS Online Proc. Libr.* **2007**, *1012* (1), 1238. https://doi.org/10.1557/PROC-1012-Y12-38.
(74) Ishizuka, S.; Okamoto, R.; Ikeda, S. Enhanced Performance of Ternary CuGaSe$_2$ Thin-Film Photovoltaic Solar Cells and Photoelectrochemical Water Splitting Hydrogen Evolution with

Modified p–n Heterointerfaces. *Adv. Mater. Interfaces* **2022**, *9* (25), 2201266. https://doi.org/10.1002/admi.202201266.

(75) Ikeda, S.; Okamoto, R.; Ishizuka, S. Enhancement of the Photoelectrochemical Properties of a $CuGaSe_2$-Based Photocathode for Water Reduction Induced by Loading of a Cu-Deficient Layer at the p–n Heterointerface. *Appl. Phys. Lett.* **2021**, *119* (8), 083902. https://doi.org/10.1063/5.0060494.